SHOCK DIFFRACTION COMPUTATIONS OVER COMPLEX STRUCTURES

Andrew Mark
Ballistic Research Laboratory
U.S. Army Armament Research and Development Command
Aberdeen Proving Ground, Maryland 21005

and

Paul Kutler, Chief
Applied Computational Aerodynamics Branch
NASA Ames Research Center
Moffett Field, California 94035

This work contains the results of a study aimed at the development of two- and three-dimensional numerical procedures for computing the flowfield generated by the interaction of a blast wave and a rigid body. A number of numerical procedures were applied to two-dimensional problems including both implicit and explicit algorithms. Each was tried on the blast wave-cylinder interaction problem. MacCormack's method with added fourth-order dissipation yielded the best results and was then applied to the blast wave-truck interaction problems in two dimensions. MacCormack's method was also used in three dimensions to determine the flowfield that results when a blast wave strikes a rectangular parallelepiped at an arbitrary angle. Both the two- and three-dimensional computations were compared with experiments in a number of ways. Two dimensional density contours show qualitative agreement for shock front location and Mach stem formation with spark shadowgraphs taken in a shock tube. Pressure-time histories indicate good quantitative agreement between theory and experiment both in two- and three-dimensions.

INTRODUCTION

The accurate prediction of the effects of blast waves encountering vehicles and structures is essential in the design, survivability, and hence effectiveness of these configurations. Detailed experimental blast wave interaction data is both costly and difficult to obtain. Moreover, these experiments frequently do not provide a complete picture of the blast wave interaction flowfield. Actual experiments, in fact, only yield pressure data at a few selected points on the models. As a consequence essential design parameters are often difficult to define.

Design information for the kind of blast wave-vehicle encounter as pictured in Fig. 1 may be obtained experimentally in several ways. In one approach a large explosive charge is detonated near an instrumented vehicle or structure enabling direct measurements to be taken. This approach, while realistic, is costly, results in few data points, and frequently provides little understanding of the important flowfield phenomena. Another approach is to place a model of

the target inside a shock tube. In this case, better control can be provided and the experimental cost is less. Nevertheless, the experiments are still limited in their range of applicability as a result of scaling, shock tube wall effects, realistic wave shapes and flow duration.

As an alternative to the experimental description of the blast wave interaction phenomenon, one can use computational fluid dynamics. This is the approach adopted here. Accurate finite difference simulations offer the possibility of providing design data at a relatively low cost. Such a simulation provides a complete flowfield description that is essential to a fundamental understanding of the fluid mechanics and a necessity for an effective structural design. The numerically generated flowfield data can then be integrated to yield other vital information such as the total loads, center of pressure, and overturning moments.

In the past second-order finite-difference procedures have been used by Kutler, et al. (See References 1 and 2) to solve simple shock-diffraction problems involving both regular and Mach reflections of the incident shock. In these cases all discontinuities were fit, i.e., treated as sharp discontinuities. Blast wave encounter problems with two-dimensional wedges and three-dimensional cones in supersonic flight have been solved by Kutler, et al. (See References 3 and 4) again using second-order finite-difference procedures. In these instances a "shock-capturing" philosophy was employed and resulted in an accurate description of the so-called "shock-on-shock" problem.

In the present paper, these "shock-capturing" flowfield simulation techniques have been adapted to the blast-wave interaction problem. Only inviscid flow problems have been considered, but both complex two-dimensional and simple three-dimensional geometric configurations have been used as targets.

GOVERNING EQUATIONS

Several assumptions are made in the present study of blast wave encounters with targets. The first is that the blast wave is assumed to be planar relative to the target and that conditions behind the wave can be adequately and consistently described. Secondly, viscous effects are ignored. Finally, any effects which result from radiative heating on the target are assumed negligible, and a perfect gas equation of state is employed.

Under the above assumptions, the governing partial differential equations are the unsteady Euler equations. To permit the mapping of two- or three-dimensional complicated physical regions into rectangular or cubical computational domains respectively, the following independent variable transformation is employed:

$$\tau = t; \quad \xi = \xi(t, x, y, z); \quad \eta = \eta(t, x, y, z); \quad \zeta = \zeta(t, x, y, z) \qquad (1)$$

Because the above transformation maps the body and outer boundary surfaces onto constant coordinate lines and planes, application of the boundary condition procedures is facilitated. The above transformation also permits the clustering of grid points in the vicinity of the body.

Under this transformation, the governing partial differential equations in strong conservation law form become

$$q_\tau + E_\xi + F_\eta + G_\zeta = 0 \qquad (2)$$

where the flux vectors E, F, G of Eq. (2) assume the form

$$E = \begin{bmatrix} \rho U \\ \rho uU + \xi_x p \\ \rho vU + \xi_y p \\ \rho wU + \xi_z p \\ (e + p)U - \xi_t p \end{bmatrix} \quad F = \begin{bmatrix} \rho V \\ \rho uV + \eta_x p \\ \rho vV + \eta_y p \\ \rho wV + \eta_z p \\ (e + p)V - \eta_t p \end{bmatrix} \quad G = \begin{bmatrix} \rho W \\ \rho uW + \zeta_x p \\ \rho vW + \zeta_y p \\ \rho wW + \zeta_z p \\ (e + p)W - \zeta_t p \end{bmatrix} \tag{3}$$

where $U = \xi_t + u\xi_x + v\xi_y + w\xi_z$, $V = \eta_t + un_x + vn_y + wn_z$, and $W = \zeta_t + u\zeta_x + v\zeta_y + w\zeta_z$ are the contravariant velocity components without metric normalization.

In the conserved variables of Eq. (2) p represents the pressure, ρ the density, u, v, and w the three Cartesian velocity components, and e the total energy per unit volume. For an ideal gas, the pressure, density, and velocity components are related to the energy by the following equation:

$$e = \frac{p}{\gamma - 1} + \rho \frac{u^2 + v^2 + w^2}{2} \tag{4}$$

The metrics required by Eq. (3) in general are not known analytically and must be evaluated numerically. Details for this procedure are given in Reference 5.

NUMERICAL ALGORITHMS

The transformed governing equations (Eq. (2)) were solved by both explicit and implicit finite-difference procedures. These schemes included MacCormack's[6] explicit method with an additional fourth-order dissipation term, Beam and Warming's[7,8] implicit method in the delta-form, and Steger and Warming's[9] explicit upwind scheme. MacCormack's scheme captured the shock within the least number of grid points and consumed the least amount of machine time, and therefore, it is the only procedure presented here. The others can be found in Reference 5.

MacCormack's method is a second-order, noncentered predictor-corrector scheme and appears as follows:

$$\left.\begin{aligned} \bar{q} &= q^n - \Delta t(\Delta_\xi E^n + \Delta_\eta F^n + \Delta_\zeta G^n) \\ q^{n+1} &= \tfrac{1}{2}[\bar{q} + q^n - \Delta t(\nabla_\xi \bar{E} + \nabla_\eta \bar{F} + \nabla_\zeta \bar{G}) + \epsilon D^n] \end{aligned}\right\} \tag{5}$$

where $\bar{E}$ implies that the flux vector E is evaluated using elements of the predicted value $\bar{q}$, and Δ and ∇ are the standard forward and backward difference operators. The quantity D represents a fourth-order dissipation term in all three directions whose effect is governed by the dissipation constant ϵ.

GRID GENERATION

The generalized coordinate transformation given by Eq. (1) permits the use of grids based not only on standard coordinate systems such as cylindrical or spherical but also numerically generated grids such as those obtained by solving elliptic partial differential equations. In this study both analytically and numerically determined grids were used to discretize the physical regions of interest.

For two-dimensional targets consisting of cylinders and rectangles, an analytically described mesh based on a cylindrical-like coordinate system is employed (see Figs. 2a and 2b). Points can be clustered near the body for better resolution by using an exponential function.

In order to discretize an arbitrary two-dimensional shape such as a truck and its surrounding flowfield, a numerically generated grid was used (see Fig. 2c). The partial differential equations used for this process are elliptic and satisfy a maximum principle. The technique for generating these grids was obtained from R. L. Sorenson at NASA's Ames Research Center and was a result of a paper by Steger and Sorenson.[10] Details of the mesh generation procedure can be found in that paper, but suffice it to say that the method can treat arbitrary bodies and outer boundaries with clustering near the body.

For the three-dimensional problem, the flowfield resulting from the interaction of a blast wave and a rectangular parallelepiped was desired. Discretization of this flowfield was accomplished using a spherical-type grid as shown in Fig. 3.

BOUNDARY AND INITIAL CONDITIONS

Two types of computational boundaries were considered; those across which there is no mass flow (impermeable surfaces) and those across which there is mass flow (permeable surfaces). Impermeable boundaries include solid walls, planes of symmetry, and slip surfaces whereas permeable boundaries include shock waves, porous walls, and inflow or outflow boundaries.

In the blast wave interaction problems of interest here, boundary condition procedures are required at the body, the planes of symmetry, and along the outer boundary. For inviscid flows, the boundary condition at the surface of a body requires flow to be tangent to the body. This implies that the velocity component V of Eq. (3) must be equal to zero at the body. In order to simulate this numerically, the image plane concept is used. By employing this concept, an image line of nodal points is established which falls one mesh interval inside of the body (see Figs. 2 & 3). Flow variables along this line are obtained by use of the flow variables at the body and the adjacent flowfield interior points, both at the previous time step. The flow variables for the new time step at the body can now be obtained by the same numerical algorithm that was used for the interior points, and hence with the use of the implicit procedure, the body points are also updated implicitly. The details of this procedure for both the two- and three-dimensional cases are given in Reference 5.

To numerically simulate the ground plane (plane of symmetry) in both the two- and three-dimensional problems, the reflection principle is employed. In this approach the pressure, density, energy, and tangential velocity components, are treated as even functions with respect to the ground plane while the normal velocity component is treated as an odd function.

RESULTS AND DISCUSSIONS

In this section numerical results are presented which describe the interaction of a blast wave with a body. In two-dimensions, a comprehensive set of results is presented for the blast wave-cylinder interaction while partial results are presented for the blast wave-truck interaction. In three-dimensions partial results are also presented for the blast wave parallelepiped interaction problem.

Numerical and experimental results for the blast wave-cylinder interaction problem are presented in several ways. In Fig. 4a computed pressure-time histories are compared with experimental results obtained by Pearson et al[11] at the Ballistic Research Laboratory. The inset in each figure depicts the measuring

station of the transducer. The blast wave passes over the cylinder from left to right. In each case, the smooth curve is the computed result while the oscillatory curve is the measurement. The oscillations represent excursions from true values due to transducer ringing, local unsteadiness due to model oscillations, general flow anomalies, etc. A sample of the more interesting cases with significant wave structure are shown (θ = 45°, 135°, 180°). All the locations (except for 180°) have a similar structure. A sharp rise in the pressure signifies the arrival of the incident blast wave at the measuring station. This is followed by an exponential-like decay and a second, more "smeared" jump to a plateau value. The delays from t = 0 on the abscissa represent the time before the shock arrived at the sampling station. The results can be more fully explained with the help of Figs. 4b, computed isopycnics, and 4c, spark shadowgraphs (obtained by Vandromme[12]). Interesting results develop as the shock encounters the cylinder and passes over it. A triple point and Mach Stem appear partway up the windward side of the cylinder as is clearly seen in both the computed isopycnics and the shadowgraphs. The contact surface emanating from the triple point (as seen in Fig. 4c) is not reproduced in the isopycnic plots of 4b. This is because of inadequate resolution of the computational grid. Better results would be obtained with an increase in the number of grid points or an adaptive gridding scheme. As the primary shock continues toward the rear of the cylinder, it eventually reflects and is propagated upstream. As this reflected shock arrives at a measuring station, it gives rise to the second "smeared" jump in Fig. 4a. The smeared nature of the jump is manifest in viscous effect near the surface which now begin to make their effects felt. The discrepancy in the pressure amplitude in the bottom figure of 4a and the latter half of the top two figures is also attributable to viscous effects. These effects were neglected in the computation.

The interaction of a blast wave with a truck for intermediate times is shown in Fig. 5 in the form of pressure contours. For this case the grid size consisted of 32 points in the j-direction (along the body) and 25 points in the k-direction (normal to the body). The blast wave had a strength of 34.5 kPa overpressure. Figure 5a shows the reflected blast wave from the front of the truck while Fig. 5b shows a reflected wave from the windshield. In Fig. 5c the blast wave is beginning to expand over the cab of the truck while the reflected waves from the front and windshield move away from the vehicle. This particular calculation does demonstrate the versatility of the arbitrary body mesh generator and shock-capturing ability of MacCormack's method for computing complicated flowfields.

The three-dimensional interaction of a blast-wave with a rectangular parallelepiped was computed using MacCormack's method with fourth-order smoothing. For this calculation the grid consisted of 54 points in the j-direction or around the body, 24 points in the k-direction, and 16 points in the l-direction, or between the body and the outer boundary (see Fig. 3).

Numerical results were obtained for which experimental data was available. The experimental data was obtained by placing pressure gages at various positions on the model and recording the time histories of the pressure as it was struck by the blast wave (see Fig. 3).

The initial conditions for this case consisted of a blast wave Mach number of 1.14, freestream pressure of 101.33 kPa, and angle of incidence α of 52.5°. The distance r_{bw_i} from the origin to the blast wave (see Fig. 3) was 4.91.

The results of this first calculation are shown in Fig. 6 where the pressure in kilo-Pascals is plotted as a function of time in milliseconds for three stations. The solid dots shown on each of the curves in Fig. 6 is the experimental data. The agreement is acceptable and can be made much better with better grid resolution.

REFERENCES

1. Kutler, P. and Shankar, V. S. V., "Diffraction of a Shock Wave by a Compression Corner; Part I-Regular Reflection," presented at the AIAA 9th Fluid and Plasma Dynamics Conference, San Diego, CA, July 14-16, 1976. AIAA Journal; Vol. 15, No. 2, February 1972, pp. 197-203.

2. Shankar, V., Kutler, P., and Anderson, D. A., "Shock Wave by a Compression Corner; Part II-Single Mach Reflection," AIAA Paper 77-89, presented at the AIAA 15th Aerospace Sciences Meeting, Los Angeles, CA, January 24-26, 1977. AIAA Journal, Vol. 16, No. 1, pp. 4-5, January 1978. Also NASA Technical Memorandum TM-73, 178.

3. Kutler, P. and Sakell, L., "Two-Dimensional, Shock-on-Shock Interaction Problem," AIAA Journal, Vol. 13, No. 3, pp. 361-367, March 1975.

4. Kutler, P. and Sakell, L., "Three-Dimensional, Shock-on-Shock Interaction Problem," AIAA Journal, Vol. 13, No. 10, pp. 1360-1367, October 1975.

5. Kutler, P. and Fernquist, A. R., "Computation of Blast Wave Encounter with Military Targets," Flow Simulations, Inc. Report No. 80-02, April 1980.

6. MacCormack, R. W., "The Effect of Viscosity in Hypervelocity Impact Cratering," AIAA Paper 69-354, Cincinnati, Ohio, 1969.

7. Beam, R. and Warming, R. F., "An Implicit Factored Scheme for the Compressible Navier-Stokes Equations," AIAA Paper 77-645, 1977.

8. Warming, R. F. and Beam, R., "On the Construction and Application of Implicit Factored Schemes for Conservation Laws," SIAM-AMS Proceedings, Vol. 11, Proceedings of the Symposium on Computational Fluid Mechanics, New York, 1977.

9. Steger, J. L. and Warming, R. F., "Flux Vector Splittings of the Euler Equations in Conservation Law Form," NASA TM-78605, July 1979.

10. Steger, J. L. and Sorenson, R. L., "Automatic Boundary Clustering in Grid Generation with Elliptic Partial Differential Equations," submitted to the Journal of Computational Physics.

11. Pearson, R. J., Wisniewski, H. L. and Szabados, P. D., "Synergism in Nuclear Thermal/Blast Loading," Proceedings of the 7th International Symposium on Military Application of Blast Simulation, Ralston, Alberta, Canada, July 1981.

12. Vandromme, D., "Contribution to the Study of a Diffraction Pattern of a Plane Shock Wave Around a Cylinder," Secondary Thesis, Von Karman Institute for Fluid Dynamics, June 1980.

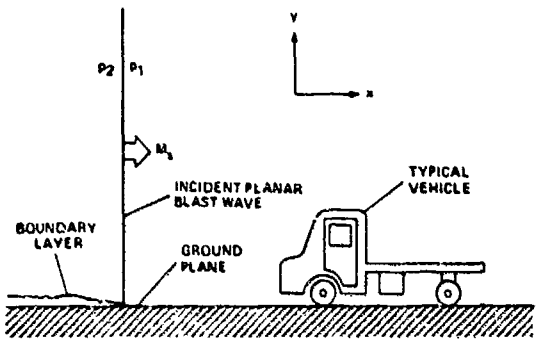

Figure 1. Blast Wave-Vehicle Interaction Problem

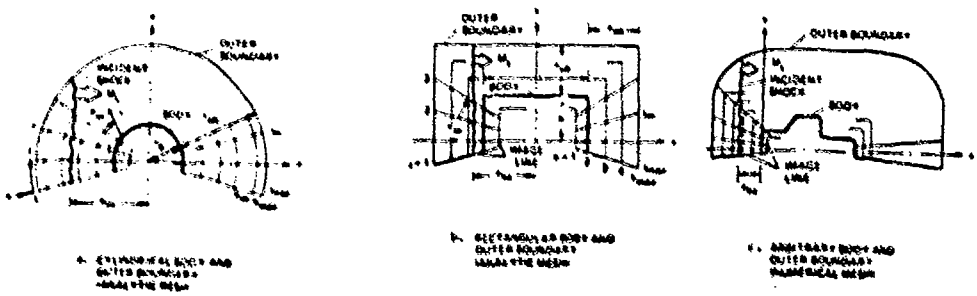

Figure 2. Description of Grids Used in Two-Dimensional Problem

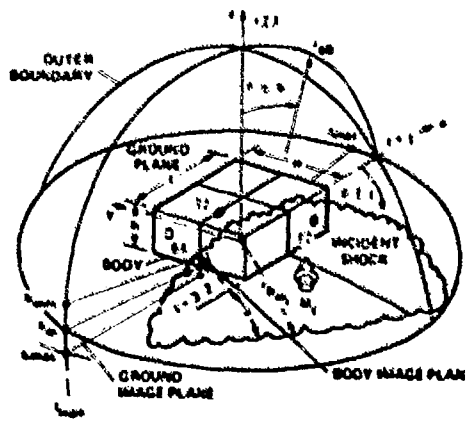

(x_0, y_0, z_0) - DISPLACEMENT OF SPHERICAL OUTER BOUNDARY ORIGIN

Figure 3. Description of Grid Used in Three-Dimensional Problem

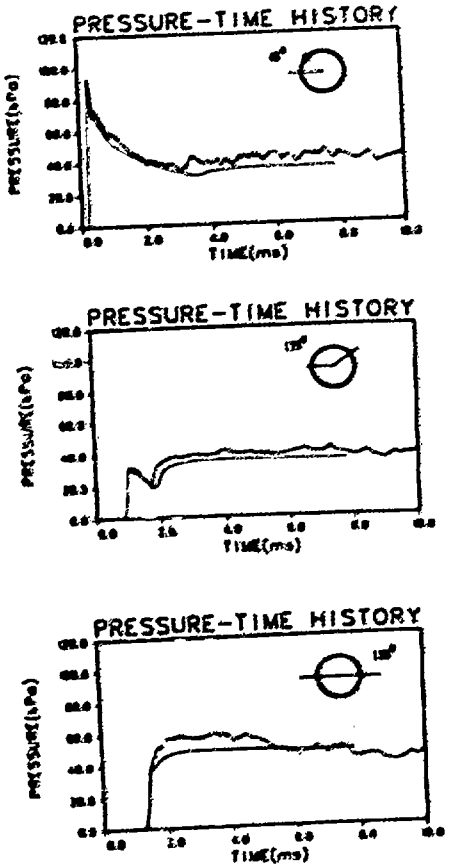

(a) Pressure-Time History for Shock Strength of 1.3 kPa.

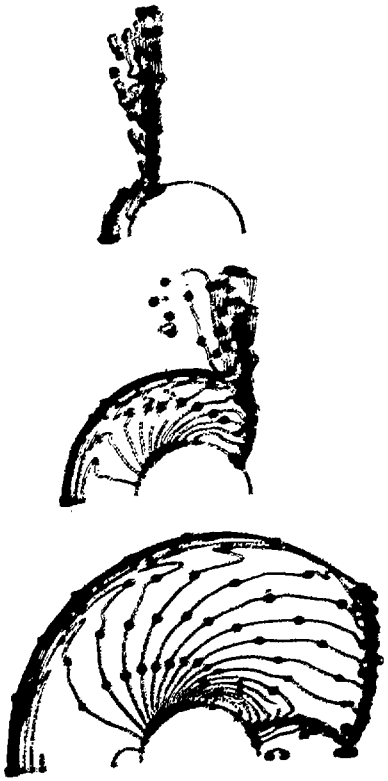

(b) Computation

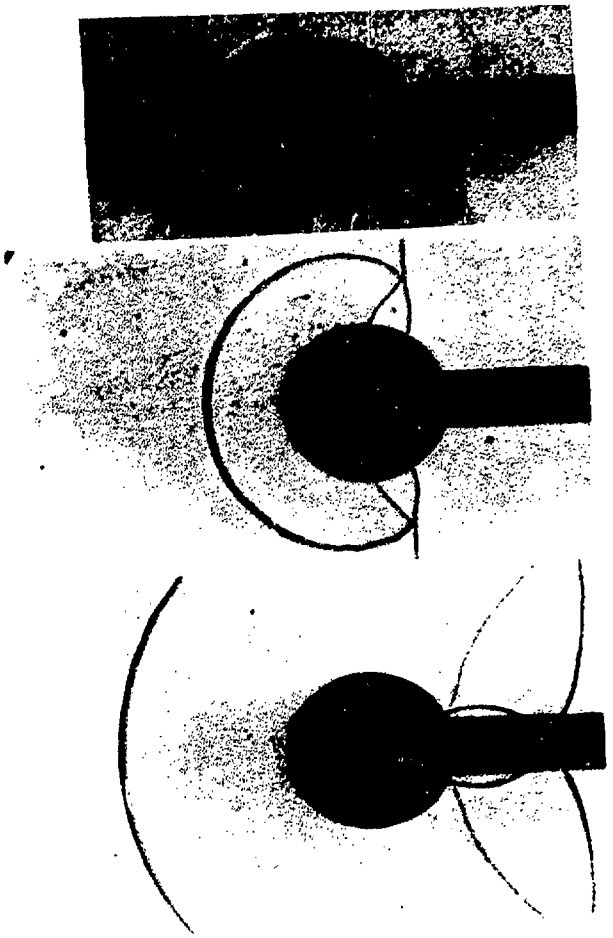

(c) Spark Shadowgraphs by Vandromme[12]

Figure 8 Short Wave, Cylinder Encounter, $M_s = 1.17$

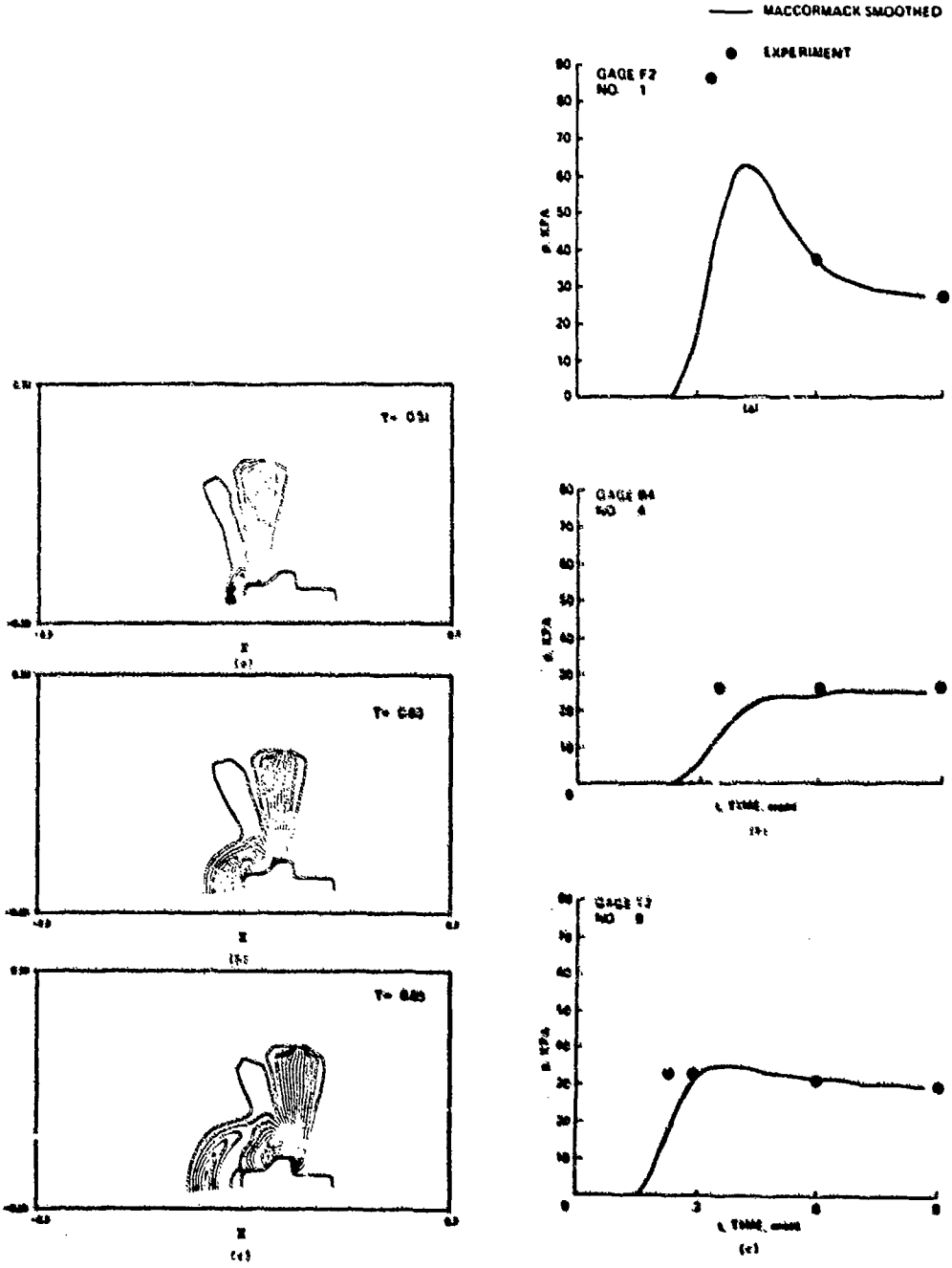

Figure 5. Pressure Contours of Blast Wave-Cubicle Interaction; $M_s = 1.10$

Figure 6. Surface Pressure Distribution on a Rectangular Parallelepiped as a Function of Time for Various Gage Positions; $M_s = 1.13$, $\alpha = 52.5°$.